International Journal of Operations Research

International Journal of Operations Research Vol. 7, No. 4, 51−65 (2010)

An Efficient Approximation for Refining Organ Geographic Distribution in the U.S. Liver Transplantation and Allocation System

Yu Teng [1] **and Nan Kong** [2,*]

[1, 2] Weldon School of Biomedical Engineering, Purdue University

206 S. Martin Jischke Drive, West Lafayette, IN 47907

Received August 2010; Revised November 2010; Accepted December 2010

Abstract—Liver transplantation and allocation has been a contentious issue in the United States for decades. Two main challenges in achieving efficient sharing are 1) significant geographic imbalance between donor supply and patient demand, and 2) rapid quality decay of livers. At present, when deciding which immunologically compatible patients should be given higher priorities for donor livers, priorities are given to local patients first, then patients in nearby areas of the procurement site (*region*), and finally remaining patients from the entire nation. The allowance of allocating livers in nearby areas before making them available to the entire nation ensures that good candidates can receive high-quality liver transplants. In this paper, we present a deterministic sequential matching model to evaluate the impact of allocation region design. We show that the developed model is a good approximation to the real system and it facilitates the numerical analysis of liver geographic distribution. We make recommendations on how geographic configuration of the liver allocation system may be modified to improve post-transplant outcomes.

Keywords — Liver transplantation and allocation, proportional allocation, graph partitioning, greedy heuristic.

1. INTRODUCTION

End-stage liver disease (ESLD) is the 12th leading cause of death in the United States. Approximately 30,000 people die annually due to the disease (Xu et al., 2009). Many ESLD patients with acute conditions have a life expectancy of only one week without a transplant (UNOS, 2010a). At present, the only viable therapeutic option for almost all ESLD patients is receiving a cadaveric liver transplant, i.e., the liver is typically procured after the donor is dead. Unfortunately, there is a huge discrepancy between liver supply and patient demand. Furthermore, due to rapid quality decay, many procured livers become unaccepted for transplant when they arrive at transplant operation sites. Currently, there are approximately 16,000 patients waiting for liver transplants. Furthermore, in recent years, more than 11,000 new patients are listed to the waiting list annually, whereas only around 7,000 cadaveric livers are procured annually (UNOS, 2010c). Many patients die before they ever receive liver offers. Therefore, it is critical to design a liver allocation system that facilitates efficient sharing. In Table 1, we report statistics in recent years on cadaveric liver procurement, ESLD patient listing, pre-transplant deaths, and transplants performed. As in many scarce resource allocation problems, a key challenge in liver allocation is developing guidelines to determine who should be allocated with the resource when it becomes available. In this work, we focus on cadaveric liver transplantation and allocation and refer to it simply as liver transplantation and allocation. It is worth noting that a small percent of patients have the chance of receiving living donor transplants. However, we do not think such exclusion will significantly affect our analysis. For an introduction on living donor transplantation, we refer to Marcos et al. (1999).

Organ procurement organizations (OPOs) are important members in the U.S. liver transplantation and allocation system. Each OPO presides over a designated service area in patient registration, organ procurement, donor/recipient matching, and organ transport arrangement between the procurement and recipient sites. One or

* Corresponding author's email: nkong@purdue.edu

several transplant centers are associated with each OPO. Currently, the entire U.S. is divided into 58 OPO designated service areas (See Figure 1). The service area of each OPO varies from part of a state to several states combined. The United Network for Organ Sharing (UNOS) is the national-level organization that provides guidelines to OPOs on the allocation process and maintains a database containing patients' clinical and demographic characteristics needed for matching and prioritization.

Table 1: Liver Transplantation and Allocation Data (UNOS, 2010c)

	2004	2005	2006	2007	2008	2009
Cadaveric Donor Livers	6,319	6,693	7,017	6,936	6,752	6,738
Waiting List Additions	10,640	10,986	11,036	11,081	11,176	11,255
Cadaveric Donor Transplants	5,848	6,121	6,363	6,228	6,070	6,101
Patient Death While Waiting	1,926	1,935	1,811	1,641	1,549	1,510

Figure 1: OPO Service Areas (IoM, 1999)

There are two classes of outcomes that are used to measure the performance of the allocation system: pre- and post-transplant outcomes. Outcomes at the pre-transplant phase include pre-transplant patient mortality risk, waiting time, waitlist length, etc. Outcomes at the post-transplant phase include post-transplant patient survival rate, quality-adjusted life years (QALYs), duration of transplanted liver being functioning, etc. In this research, we focus on post-transplant outcomes. Studies (e.g., Piratvisuth et al., 1995; Totsuka et al., 2002) show that an important factor on post-transplant outcomes is the time interval between the liver is procured from the donor's body and it is implanted into the recipient's body, termed "cold ischemia time" (CIT) (IoM, 1999; UNOS, 2010a).

Several studies further suggest that post-transplant survival rate is low if the liver procurement site is far from where the patient resides (Stahl et al., 2008; Totsuka et al., 2002). Maximum acceptable CIT for liver transplant is 12 - 18 hours (IoM, 1999). Therefore, an allocation system that only allows liver sharing with nearby transplant centers is likely to achieve greater transplant efficiency for the entire system. Such an allocation scheme has been advocated at the state level (Haymarket Media, Inc., 1998; State Legislatures, 1999; The Economist Newspaper Ltd., 1998; Walter, 1998). However, such a scheme was criticized for being unethical due to the fact that livers may not be transplanted to the patient whose disease is the most severe and who needs the transplant the most, and being inequitable due to the fact that there is significant geographic disparity both on the supply and demand sides in the system. The U.S. federal government advocates an allocation system with complete national sharing based on medical urgency (Henderson, 2000).

As a compromise between the federal government and the states, a three-tier hierarchical allocation system was introduced by UNOS in the late 1990s with the inclusion of regional-level allocation between allocation within each OPO service area and nationwide allocation. With a few exceptions, the current UNOS liver allocation process uses the following hierarchy. Once a liver is procured by an OPO, it is first offered to an immunologically compatible candidate that is registered on the waiting list of the procurement OPO. If the liver cannot find a compatible candidate or is not accepted by any compatible candidate who has been made the offer, it is offered to a larger area, or region. Currently, the entire country is divided into 11 regions (see Figure 2). If a liver cannot be matched nor accepted for transplant in the procurement region, it is offered nationwide. We term the three levels of geographic proximity G_1 (local), G_2 (regional), and G_3 (national), respectively.

Intuitively, when a liver is procured by an OPO, it is more likely to be transplanted at the regional level if the OPO is contained in a large region as opposed to a small region. However, a large region may force many procured livers to travel farther, which in turns reduces the quality of the liver and leads to negative consequences on post-transplant system outcomes. Hence, a major contention in liver allocation is rooted at determining the

composition of allocation regions, which is essentially determining the membership of each OPO in candidate regions. We define a regional configuration to be a partition of the entire country into a number of allocation regions. Note that in a regional configuration, each OPO is only contained in one region.

Figure 2: Current Region Map (UNOS, 2010a)

In this paper, we develop a deterministic sequential allocation model to evaluate alternative regional configurations withtween 6 and 40. The current prioritization guideline stratifies patients into three groups according to their medical urgency. For convenience, we call the three patient groups M_1 (acute), M_2 (MELD score ≥ 15), and M_3 (MELD score < 15).

With the two aforementioned classification criteria, the current allocation guideline stratifies immunologically compatible patients into nine classes. Figure 3 illustrates the nine classes and the current allocation priorities. The three circles represent three levels of geographic proximity and three sections represent three classes of medical urgency. The arrow indicates the sequence of patient classes receiving the liver. Within each acute patient class, compatible patients are ranked by their waiting times. Patients with longer waiting times are given higher priorities. Within each chronic patient class, compatible patients are f respect to post-transplant system outcomes. With a significant and steadily increasing percentage of transplants being performed with procured livers allocated at the regional level, we believe that it is important to explore the possibility of refining the current regional configuration. Several stochastic simulation models can be used to improve system efficiency of liver transplantation and allocation in the U.S. However, these models suffer computational burden when attempting to design optimal allocation policy and system. Our model, on the other hand, provides a good deterministic proxy that substantially reduces the computation required for the optimization without losing much realism and accuracy. Therefore, we believe that our work has the potential to be adapted in future liver allocation system optimization in the U.S. and worldwide. Furthermore, we do not propose a complete overhaul of the current U.S. allocation system. Instead, we only suggest modest regional reconfiguration while maintaining the current three-tier allocation framework. This greatly increases the likelihood of eventual implementation, as the current hierarchy is widely accepted after decades of contention.

In addition to geographic proximity, medical urgency is an equally important criterion considered in the current UNOS liver allocation. When measuring medical urgency, an ESLD patient is first classified as an acute patient or a chronic patient. Acute patients have a life expectancy of a week on average and thus have the greatest medical need. Compared to acute patients, chronic patients can normally live longer. To measure their medical urgency, UNOS applies the Model for End-Stage Liver Disease (MELD) score. This score is a combination of three laboratory values (bilirubin, creatinine, and international normalized ratio for prothrombin time), and intended to predict the 3-month pre-transplant mortality risk for ESLD patients on the waiting list (Kamath et al., 2001; Wiesner et al., 2001). MELD scores are integers be irst ranked by their MELD scores and then by their waiting times.

In our model, we estimate how likely each liver will be allocated to each step in the current allocation process with the incorporation of patient acceptance/rejection decisions. With the likelihood estimate for each procured liver, we further estimate the expected post-transplant outcomes generated by the transplant. With the occurrence of a patient receiving transplant and being removed from the waiting list, we also update the waiting list periodically in the model. Finally, we aggregate the expected outcomes over the sequentially occurring transplants. For each procured liver, different regional configurations lead to different allocations. Thus, different configurations achieve different aggregate system outcomes over a period of time. We estimate the model parameters based on historic liver procurement and patient waiting data.

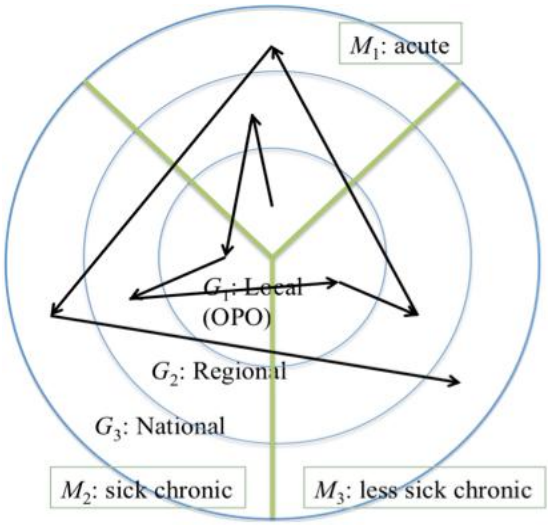

Figure 3: Current Sequential Allocation Process (UNOS, 2010b)

Our model provides a good proxy to the current U.S. liver allocation system. More importantly, it gives us the opportunity to refine the current allocation policy efficiently. With the model, we can efficiently identify regional configurations that achieve promising outcomes. Although existing simulation models can be used to perform the same evaluation, they suffer from huge computational burden. Therefore, it hinders allocation policy maker from refining regional configurations and eventually designing promising ones. To the best of our knowledge, this work is the first that refines liver allocation region design with the consideration of the entire allocation process and with the aim of achieving better overall post-transplant outcomes. We obtain regional configurations that are superior to the current configuration, by applying a simple greedy heuristic. This superiority is verified by a liver allocation simulation model developed in Feng et al. (2010).

In recent years, we have witnessed a number of mathematical and computational studies on liver allocation decisions and analysis. We refer interested readers to Alagoz et al. (2009) and Kong (2006) for comprehensive literature reviews. Three classes of references are relevant to our work. They are works that deal with designing promising liver regional configurations, modeling waiting list dynamics, and evaluating allocation policies. Among the three classes of references, the first one has direct influence on our work.

Kong et al. (2010) developed a static allocation model (more specifically, a set-partitioning formulation) and a decomposition-based branch-and-price algorithm to analyze the effect of geographic liver allocation. Their model differs from ours in three aspects. One, the static allocation model does not incorporate patient acceptance/rejection decisions. Two, the model ignores acute patients and assumes all chronic patients identical. Three, the model only counts transplants at the regional level and partially captures the effect of national-level allocation on region redesign. Their work was motivated by a study by Stahl et al. (2005), which we believe is the first that develops a mathematical model to analyze the effect of geographic liver distribution.

Zenios et al. (2000) developed a deterministic fluid model to update the kidney transplant patient waiting list with such components as waitlist additions, waitlist removals due to receiving transplant, death, and other removal reasons. The authors studied the effect of modifying several prioritization criteria. However, geographic proximity was not studied since rapid viability decay is not a critical concern in kidney allocation.

A number of simulation models (Feng et al., 2010; Pritsker et al., 1995; Ratcliffe et al., 2001; Shechter et al., 2005; Thompson et al., 2004) have been developed with the aim of quantitatively assessing liver allocation policies. Most of these models were developed prior to the introduction of the current three-tier allocation hierarchy. However, many of them can be adapted to evaluate alternative regional configurations. For example, Kong et al. (2010) and Demirci et al. (2010) used the Liver Allocation Simulation Model (LASM) developed by Shechter et al. (2005) to confirm the superiority of the proposed regional reconfigurations. In this work, we use the simulation model developed by Feng et al. (2010) to confirm the superiority.

The remainder of the paper is organized as follows. In Section 2, we develop a deterministic model to estimate the post-transplant outcomes over a sequence of procured livers that are offered along the current allocation process. In Section 3, we present our model parameter estimation and report our model validation. In Section 4, we present a simple greedy heuristic to identify promising regional configurations and report our numerical findings. In Section 5, we draw conclusions of the work and outline future research directions.

2. A SEQUENTIAL LIVER MATCHING MODEL

In this section, we develop a deterministic liver allocation model and embed it in the regional configuration optimization problem. We first estimate the likelihood that a procured liver is allocated at each of the nine steps along the allocation process. Such likelihoods are dependent upon the procured liver and the waitlisted patients at the time of procurement. We then discuss how to update the patient waiting list. Finally, we estimate the post-transplant outcomes accumulated over a period of time and present the regional configuration optimization problem. In Appendix A, we include a list of notation introduced in this section.

2.1 Sequential Matching of A Single Procured Liver

For any procured liver, denoted by *l*, we classify it by its donor immunological characteristics and procurement site. We denote the above two attributes associated with each *l* to be $B'(l)$ and $G'(l)$, respectively. Meanwhile, for any patient on the waiting list, denoted by *p*, we classify her by her recipient immunological characteristics, registration site, and medical status. We denote the above three attributes associated with *p* to be *B*(*p*), *G*(*p*), and *M*(*p*), respectively.

To check immunological compatibility between any pair of liver *l* and patient *p*, several donor and patient immunological characteristics are taken into consideration in the current system. Due to lack of data, we use ABO blood type as the sole immunological characteristic in our work. We label the four distinct ABO blood types A, B, O, and AB with 1 to 4, respectively. That is, $B'(l)$, *B*(*p*)= 1,...,4 for any *l* and *p*. For an introduction on ABO blood type compatibility, we refer to UNOS (2010a). In the current allocation system, the liver procurement site $G'(l)$ and patient registration site *G(p)* are identified with the OPO that procures the organ and performs transplant operation for the recipient, respectively. That is, $G'(l)$ = 1,...,58 and *G*(*p*) = 1,...,51. Note that there are a number of OPOs that only procure organs but do not perform transplant operations. With the current allocation guideline, the OPOs are grouped into three OPO classes $G_1(l)$, $G_2(l)$, and $G_3(l)$, as described in Section 1. We can express G_i, i = 1, 2, 3 as $G_1(l)=\{G'(l)\}$, $G_2(l)=\{k\in 1 \mid k \text{ in the same region as } G'(l)\}\setminus G_1(l)$ and $G_3(l)=I\setminus G_1(l)\cup G_2(l)$, where *I* is the set containing all OPOs. Finally, the medical status of a waiting list patient is either labeled acute or chronic. A chronic patient's medical status is further assessed by her MELD score. With the current allocation guideline, waiting list patients are grouped into three medical status classes M_1, M_2, and M_3, as described in Section 1.

Once a liver *l* is procured, we denote *C*(*l*) to be the set that contains all immunologically compatible patients on the waiting list at the time of procurement. After identifying *C*(*l*), we divide it into 9 subsets according to the current allocation guideline. We denote $C_i(l)$, i = 1,...,9, to be the 9 subsets, i.e., $U_{i=1}^{9}C_i(l)=C(l)$, with $C_1(l)$ and $C_9(l)$ being the subsets of patients that are granted with the highest and lowest priorities in the offering of *l*, respectively. For example, $C_1(l)=\{p\in C(l)\mid G(p)\in G_1(l), M(p)\in M_1\}$ and $C_9(l)=\{p\in C(l)\mid G(p)\in G_3(l), M(p)\in M_3\}$. For a complete list of the patient subsets, please see Appendix B.

To estimate the likelihood that a liver is allocated to each step along the allocation process, we make the following assumption regarding the probability that a patient accepts the offering of *l*.

Assumption 1 *In each class $C_i(l)$, i = 1,...,9, all patients have the same probability of accepting the offering of l. In addition, they make their acceptance/rejection decisions independently.*

Under the current policy, each patient and/or her transplant surgeon must make the acceptance/rejection decision on a procured liver within a short amount of time. Such a decision is primarily made based on the quality of the liver, which is highly correlated with the CIT. Since the quality can be objectively measured and accurately informed to the patients, it is fair to assume that all patients have the same acceptance probability. This tends to hold true especially for patients with similar medical statuses. Note that heterogeneous acceptance probability can be easily incorporated, which makes the model more accurate. However, this incorporation requires more personalized data than we currently have.

For each step *i* along the current process, i = 1,...,9, we denote $r_i(l)$ to be the probability that each patient in class $C_i(l)$ rejects *l*. Intuitively, a liver is more likely to be allocated within a larger pool of patients. We assume that the sequential matching process for a single procured liver within each step follows a geometric distribution with probability $r_1(l)$. Then the probability that liver *l* is allocated before or at step *i* is $1-\prod_{k=1}^{i} r_k(l)^{|C_k(l)|}$. Note that the conditional probability that all patients in class $C_i(l)$ reject l is $r_i(l)^{|C_i(l)|}$ given that *l* is offered to class $C_i(l)$. Then the likelihood that *l* is allocated at step *i*, denoted by $P_i(l)$, is as

$$p_i(l)=1-r_1(l)^{|C_1(l)|};\ i=1 \tag{1}$$

And

$$p_i(l) = \left(1 - \prod_{k=1}^{i} r_k(l)^{|C_k(l)|}\right) - 1 - \prod_{k=1}^{i-1} r_k(l)^{|C_k(l)|} = \left(1 - r_1(l)^{|C_1(l)|}\right) \prod_{k=1}^{i-1} r_k(l)^{|C_k(l)|};\ i = 1, \cdots, 9 \tag{2}$$

The above estimates imply that $P_i(l)$ is dependent upon $C_k(l)$ for $k = 1,...,i$. Hence, the estimated allocation likelihood $P_j(l)$ would change for all $j = i+1,...,9$ if $C_k(l)$ changed for any $k = 1,...,i$. One possible change is modifying the regional configuration, i.e., changing $G_2(l)$, which is the focus of this paper.

Next we estimate the likelihood that the procured liver l is allocated to a particular OPO. Knowing the transplant OPO allows us to predict CIT dependent post-transplant outcomes. Given an OPO j, we derive the probability that l is allocated to j at each step. If the allocation takes place at step $i = 1$, 3, or 5, then it is a local-level allocation and the probability is $P_i(l)$. For regional-level and national-level allocations, we make the following assumption.

Assumption 2 *For any procured liver l, if it is offered to one of the following classes $C_i(l)$, i = 2, 4, 6, 7, 8, 9, i.e., regional-level or national-level allocation, the allocation likelihood that the liver is allocated to OPO j is proportional to the number of $C_i(l)$ patients in OPO j's service area at step i.*

More formally, let $C_i(l, j)$ be the set of patients in OPO j's service area at step i when l is procured, i.e., $C_i(l, j) = \{p \in C_i(l) \mid G(p) = j\}$. Then the likelihood that the liver l is allocated to OPO j at *regional-level* step i, $i = 2, 4, 6$, denoted by $P_i(l, j)$, is as

$$P_j(l, j) = p_i(l) \frac{|C_i(l, j)|}{\sum_{k \in G_2(l)} |C_i(l, j)|} \tag{3}$$

Similarly, the likelihood that the liver l is allocated to OPO j at *national-level* step i, $i = 7, 8, 9$, is

$$P_j(l, j) = p_i(l) \frac{|C_i(l, j)|}{\sum_{k \in G_2(l)} |C_i(l, j)|} \tag{4}$$

In the real-world allocation process, waiting time serves as a tiebreaker to rank patients in each class. It is reasonable to assume that patients are registered at a rate proportional to the waiting list length in each class, and the likelihood of a patient at OPO i is the one who is being offered with the procured liver is proportional to the rate of registration at the OPO. Hence, over the long run, the proportional allocation scheme can approximate the real allocation process with consideration of waiting times.

2.2 Waiting List Update

In this section we construct a continuous-time deterministic model that provides a stylistic representation of the ESLD patient waiting list over time. The model differentiates a liver into J distinct categories, based on blood type and procurement site. Once a liver is procured at time t, based on the liver category, the model divides the ELSD population at time t into K distinct categories, based on blood type, registration site, and medical status. Additional relevant characteristics associated with donors and patients can be incorporated by creating more distinct categories. Note that the term category here is different from the term class used in Section 2.1. However, they are related. We discuss their relation later in this section.

The state of the system at time t is described by the K-dimensional column vector $(t) = (x_1(t), x_2(t), ..., x_K(t))^T$, which gives us the number of patients in each category. Transplant candidates of categories k, $k = 1,...,K$ are added to the waiting list at rate λ_k^+ per unit time. These patients depart from the waiting list due to non-transplantation reasons including death, which occurs at rate μ_k per unit time for category k patients, or liver transplantation.

A fraction $v_{jk}(t)$ indicates the likelihood that a category j liver is procured at time t and it is allocated to a category k patient. This fraction can be determined based on the derivation in Section 2.1. Let us represent liver category j by its components (j_b, j_g), where j_b and j_g indicate the blood type and procurement site, respectively. Similarly, let us represent patient category k by (k_b, k_g, k_m), where k_b, k_g, and k_m indicates the blood type, registration site, and medical status, respectively. Then for each pair (j, k), $j = 1,...,J$ and $k = 1,...,K$, we can determine $v_{jk}(t)$ by computing the likelihood that at time t, a liver l, with $j_b = B'(l)$ and $j_g = G'(l)$, is accepted by a patient p, with $k_b = B(p)$, $k_g = G(p)$, and $k_m = M(p)$.

Assumption 3 *The probability that a patient accepts each liver from the same liver category is identical. That is, for any patient class $C_i(l)$, $r_i(l)$ is a constant for all livers l that belong to the same category.*

With this assumption, we can aggregate the allocations of sequentially procured livers. Livers of categories $j = 1,...,J$ are procured at rate λ_j^- per unit time. We set $u_{jk}(t) = \lambda_j^- v_{jk}(t)$ to be the instantaneous transplantation rate of category j livers into category k patients.

The dynamics of the waiting list is described with a group of linear ordinary differential equations as:

$$\frac{d}{dt} x_k(t) = \lambda_k^+ - \mu_k x_k(t) - \sum_{j=1}^{J} u_{jk}(t);\ k = 1,...,K \tag{5}$$

The above system dynamics model is a simplified version of the model presented in Zenios et al. (2000) in that for computational tractability, our model does not model the dynamics of post-transplant patients. Some of these patients experience graft failure and rejoin the waiting list. We simply use λ_k^+ to model both first-time registered patients and relisted patients in each category k. In Section 3, we will show that this simplification presents a meaningful system proxy for comparing alternative regional configurations. The other difference between the two models is that fractions $u_{jk}(t)$ in our model are determined based on the current allocation process whereas they are modeled as control variables in Zenios et al. (2000). It is also worth noting that our model does not update each patient's health condition over time. However, the health condition update can be incorporated by modeling the patient transitions between each category k and other categories. This simplification is also with the consideration of computational tractability.

2.3 Regional Configuration Optimization

In this section we present the regional configuration optimization problem. That is, find a regional configuration such that the overall post-transplant outcome over a period of time can be maximized.

Assumption 4 *The post-transplant outcome is identical to transplants between any liver in the same liver category and any patient in the same patient category.*

Following the above assumption, we can compute the post-transplant outcome accumulated over [0, T) as

$$f = \sum_{j=1}^{J} \sum_{k=1}^{K} \int_0^T f_{jk}(t) u_{jk}(t) dt, \tag{6}$$

where f_{jk} is the predicted post-transplant outcome of a transplant between a category j liver and a category k patient, $j = 1,...,J$ and $k = 1,...,K$.

As the regional configuration changes, i.e., $G_2(l)$ changes for each l, the aggregate outcome f changes. We use $f(R)$ to denote the aggregate outcome with regional configuration R. Then the regional configuration optimization problem is presented as: $\max_{R \in \mathbf{R}} f(R)$, where $\mathbf{R}$ is the set that contains all feasible regional configurations. The regional configuration optimization problem is formulated as a set-partitioning problem. However, the utility of each partition cannot be easily computed for two reasons. One, the utility of each region is not additive to the utilities of the OPOs contained in the region. Moreover, the utility is accumulated over time and thus no closed-form expression can be written for the computation of the utility. Therefore, in addition to developing a model that carries out the utility computation procedure, we develop a local search algorithm to make the optimization problem computational tractable. For practical implementability of the solution, we in this paper only consider $R' \subset R$, which is the set such that for each $R \in R'$, every region $r \in R$ is geographically contiguous. That is, given an adjacency matrix that indicates whether any pair of OPOs are adjacent, for any two disjoint subsets $r_1, r_2 \subset r$, i.e., $r_1 \cup r_2 = r$ and $r_1 \cap r_2 = \phi$, there exist an OPO $j \in r_1$ and an OPO $j \in r_2$ such that OPOs i and j are adjacent.

3. NUMERICAL IMPLEMENTATION OF THE DETERMINISTIC MODEL

In this section we describe the numerical implementation of the deterministic sequential liver allocation model. To evaluate $f(R)$ numerically for each regional configuration $R \in R'$, we discretized the differential equations in (5) to update the waiting list at discrete time points as:

$$x_k(t+1) = x_k(t) + \lambda_k^+ - \mu_k x_k(t) - \sum_{j=1}^{j} u_{jk}(t);\ k = 1,...,k \tag{7}$$

for $t = 0,...,T-1$. Given the waiting list $x(t)$, one can determine v_{jk} for $j = 1,...,J$ and $k = 1,...,K$. With the estimated λ_k^- from historic data, one can further determine each u_{jk}. With the estimated λ_k^+, μ_k, and $x_k(t)$, one can determine $x_k(t+1)$ for $k = 1,...,K$. Therefore, given the initial waiting list condition $x(0)$, one can determine $x(t)$ for any $t = 0,...,T-1$. At each time point one can also compute f_t, the aggregate post-transplant outcome over all liver categories and patient categories. Then $f = \sum_{t=0}^{T-1} f_t$.

In our numerical studies, we set T to be the number of days during a 5-year span from the beginning of 2004 to the end of 2008. All our model parameters are estimated based on the publicly available data from UNOS (UNOS, 2010c). We set J to be $4 \times 58 = 232$ (4 distinct ABO blood types and 58 procurement sites) and set K to be $4 \times 51 \times 36 = 7344$ (4 distinct ABO blood types, 51 registration sites, and 35 distinct MELD scores plus one medical status for acute patients). We set the initial waiting list $x(0)$ to be the real waiting list on January 1st, 2004 and updated the waiting list daily during the five-year study period.

We assumed that λ_k^+, λ_k^-, and μ_k remain constant in each year but vary from year to year. To estimate λ_k^+, we first obtained the annual number of registered patients and computed the average daily patient registrations, denoted by n. We then computed the portion of category k patient registrations to the patient registrations of all categories, denoted by ρ_k^+. Then for each category $k = 1,...,K$, $\lambda_k^+ = \rho_k^+ n$. We estimated each λ_k^- and μ_k similarly. We obtained each patient's rejection probability from Alagoz (2004), which is solely dependent upon the patient's medical status.

We estimated f_{jk} for $j = 1,...,J$ and $k = 1,...,K$, as follows. As stated in Section 1, post-transplant outcomes, such as long-term graft and patient survival rates, are highly correlated with cold ischemia time. In this work, we selected average predicated patient post-transplant 1-year survival rate to be our system outcome and assumed that the predicted post-transplant 1-year survival rate is solely dependent upon the cold ischemia time. In the remainder of the paper, we call this outcome patient survival rate for simplicity. To estimate the patient survival rate of each transplant, we used the quadratic regression model in Stahl et al. (2008) where the independent variable is cold ischemia time. To estimate the cold ischemia time of each donor liver at the time of transplant, we first estimated the liver transport distance between the procurement and transplant sites. Due to lack of actual liver transport distance data, we used the straight-line distance between the procurement and transplant OPO locations, and adjusted it by the earth curvature, to estimate the liver transport distance for each recorded transplant in the UNOS data. For more detail regarding the distance calculation formula, we refer to Page 25 in Simchi-Levi et al. (2000). We then fitted the estimated liver transport distances and recorded cold ischemia times into a linear regression model. For each $j = 1,...,J$ and $k = 1,...,K$, we computed f_{jk} and constructed a $J \times K$ matrix to store the f_{jk} values *a priori*.

We compared the deterministic model with the simulation model developed in Feng et al. (2010). Our presumption here is that the simulation model faithfully represents the real-world liver allocation system, which has been established in Feng et al. (2010). Hence, this simulation of the historic transplant data is a more accurate benchmark to the deterministic model than comparing to actual data. For an introduction of the simulation model in terms of its conceptual design, parameter estimation, and model validation, please see Appendix C. For more detailed information, we refer to Feng et al. (2010). We randomly sampled 90 regional configurations from $\mathcal{R}'$, For each sampled $R \in R'$, we evaluated the patient survival rate with both the deterministic model and the simulation model. We denote $f'(R)$ to be the simulated mean patient survival rate for a regional configuration $R \in \mathcal{R}'$. We report the comparison results in a plot of $(f(R), f'(R))$ (see Figure 4). Almost all points in Figure 4 align diagonally with a relatively constant difference between $f(R)$ and $f'(R)$ for sampled regional configurations R. With a well fitted linear regression (R^2 value = 0.8561) shown in the figure, one can estimate patient survival rate with the simulation model once the survival rate is computed with the deterministic counterpart. More importantly, the deterministic model can differentiate regional configurations with respect to the patient survival rate. To demonstrate this, we conducted the following experiment. Select any pair of regional configurations R_a and R_b such that R_a and R_b are different in terms of the studied system outcome with sufficient level of statistical significance (95% confidence level). If $f'(R_a) > f'(R_b)$ and the same conclusion is drawn with the deterministic model, i.e., $f(R_a) > f(R_b)$, we count it a correct differentiation. For all sampled 90 regional configurations, 95% of pairs could be differentiated with the simulation. Among these pairs, the deterministic model could correctly differentiate 89% of pairs. We also ranked $|f'(R_a) > f'(R_b)|$ for all simulation differentiable pairs in an increasing order. Among the top 1% pairs (i.e., the pairs with the smallest $|f'(R_a) > f'(R_b)|$), the deterministic model could correctly differentiate 76% of pairs. It is worth

noting that only a few solutions involve in most of the pairs for which the deterministic model does not make the correct judgment. Recognizing this fact, to guarantee the solution quality with the deterministic model, we applied a greedy search algorithm with multiple initial starting point and evaluated multiple final local optima with the simulation. With the aforementioned level of alignment, we concluded that we could use the deterministic model and the linear regression model as a good approximation for the stochastic discrete-event simulation model. Furthermore, we concluded that we could use the deterministic model cautiously as a good surrogate in the regional configuration optimization problem. As a result, without sacrificing the solution accuracy, we greatly reduced the solution time even with a naive greedy search algorithm.

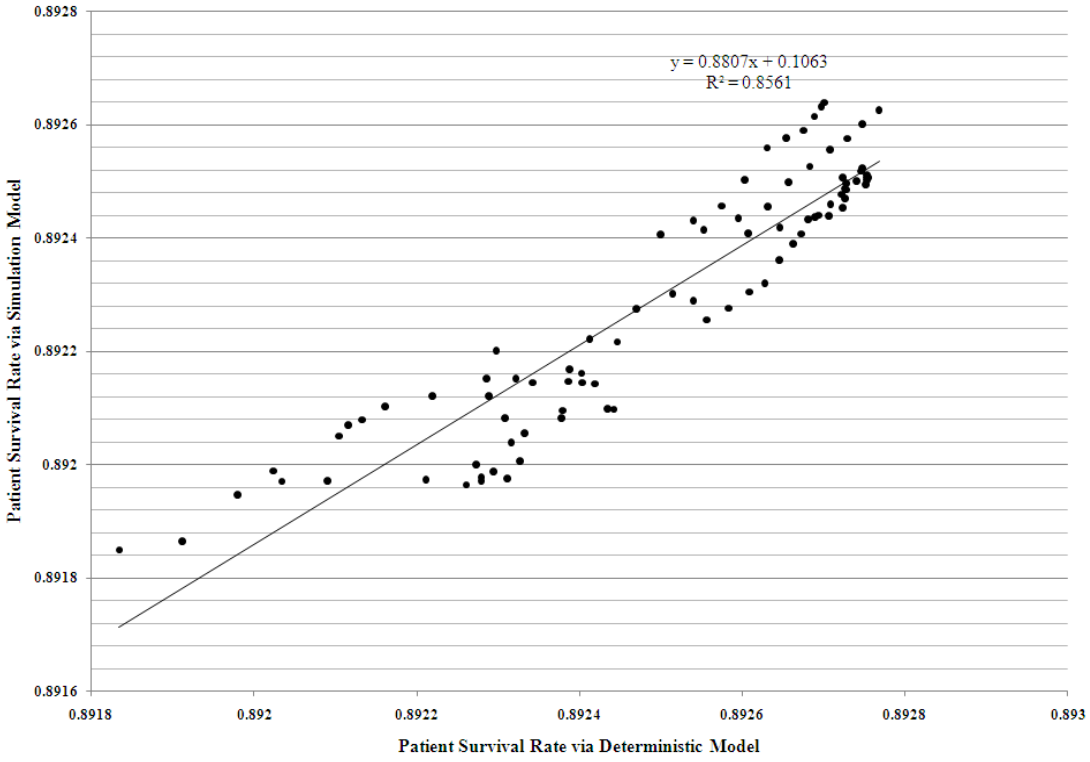

Figure 4: Comparison of the Outputs from the Deterministic Model and the Simulation Model

4. NUMERICAL STUDIES ON REGIONAL CONFIGURATION OPTIMIZATION

In this section, we first present a greedy search algorithm to solve the regional configuration optimization problem. We then report computational experiments that were conducted to identify promising regional configurations.

For any regional configuration $R \in R^{'}$, we applied move local search operations to construct the neighborhood of R. A move is defined as follows. Given any pair of regions $r, r^{'} \in R$, select an OPO $i \in r$ and move *i* from *r* to $r^{'}$. The updated regions *r* and $r^{'}$ must remain contiguous. A neighboring regional configuration $R^{'}$ is obtained after this move operation. The neighborhood of *R* is thus defined as the set containing all regional configurations that are obtained with possible move operations based on R. At each iteration of the greedy search algorithm, a neighbor R^{I} of *R* is identified that achieves the best outcome among all neighbors. Then at the next iteration, the local search is conducted based on R^{I}. The algorithm terminates when no improvement can be made with any neighbors. We present the greedy search algorithm as follows.

A Greedy Search Algorithm

Input: An initial regional configuration $R_0 \in R^{'}$ and $f(R_0)$.

Output: A regional configuration $R^{*} \in R^{'}$ that is local optimum.

Step 0. Set $k = 0$ and $f^* = f(R_0)$.

Step 1. Set $k \leftarrow k + 1$. Let $R_k' = R_k$. Set $n_k = |R_k|$. Set $i = 1$.

Step 2. For region $r_i \in R_k'$, perform the move local search operation on each OPO in r_i as follows.

Select each OPO $j \in r_i$.

1. For each region $r'_i \in R_k'$ with $r'_i \neq r_i$, set $r_i \leftarrow r_i \setminus \{j\}$ and $r' \leftarrow r' \cup \{j\}$. Then update R_k' accordingly. If R_k' is contiguous and $f(R_k') > f^*$, then set $f^* = f(R_k')$ and $R_k^* = R_k'$. Loop through all regions $r' \in R_k'$ with $r' \neq r_i$.

2. Set $r_i \leftarrow r_i \setminus \{j\}$ and $R_k' \leftarrow R_k' \cup \{j\}$. (i.e., one additional region in R_k' with only OPO *j*). If R_k' is contiguous and $f(R_k') > f^*$, then set $f^* = f(R_k')$ and $R_k^* = R_k'$.

Loop through all OPOs in r_i.

Step 3. Set $i \leftarrow i+1$. If $i > |n_k|$, go to Step 4. Otherwise, return to Step 2.

Step 4. If $f^* > f(R_k)$, $R_k \leftarrow R_k^*$ and go to Step 1. Otherwise, STOP and output R_k.

There are two cases where an inferior local optimum may occur. One, the greedy search algorithm reaches an inferior local optimum with respect to *f*. Two, although the local optimum is reasonably good with respect to *f*, it is inferior with respect to f'. To avoid the above two cases, we ran the greedy search algorithm with multiple initial regional configurations and simulated the regional configurations that correspond to a number of better local optima. We selected the regional configuration that achieves the best simulated result. In our numerical studies, we started the greedy search algorithm with 10 randomly selected regional configurations and simulated the 5 regional configurations that correspond to the 5 top local optima. We selected the regional configuration that achieves the best simulated patient survival rate among the 5 top candidates. We also imposed a restriction with which we only considered contiguous regional configurations with exactly 11 regions (i.e., only executed the first part of Step 2 in the greedy algorithm) and conducted the same experiment.

Table 2 reports the comparison of the simulated patient survival rates between the two identified promising regional configurations and the current configuration. In the table, we denote C_1, C_2, and C_3 to be the current regional configuration, the best configuration without specification on the number of regions, and the best configuration with exactly 11 regions, respectively. In addition to comparing the regional configurations with respect to average predicted 1-year patient survival rate over all transplants, we compared the regional configurations with respect to average predicted 1-year patient survival rate over all regional- and national-level transplants. The comparative results show that the two identified regional configuration outperform the current one with sufficient level of statistical significance. Furthermore, such superiority enlarges in terms of the survival rate of patients receiving regional- and national-level transplants. It is worth noting that regional reconfiguration only slightly affects the distribution of procured livers at local level. This implies that the improvement on patient survival rate is mainly due to more efficient geographic distribution of procured livers to larger areas. Figure 5 shows the two regional configurations. When there is no specification on the number of regions in a regional configuration, small regions tend to be formed to guarantee that more procured livers are allocated to nearby patients even if they are not local. We also ran the simulation for the regional configuration containing only single-OPO regions. Our simulation results show that such a configuration appears to be inferior to the identified regional configurations. This implies that it is still required to balance liver supply and patient demand.

Table 2: Comparing the Identified Regional Configurations with the Current Configuration

		Mean Diff.	T-Value	P-Value
C_2 *vs.* C_1	Overall	0.00071	18.73	0
	w/o Local	0.00249	7.57	0
C_3 *vs.* C_1	Overall	0.00051	13.21	0
	w/o Local	0.00331	13.96	0

Figure 5: Promising Regional Configurations Identified with the Deterministic Model and Greedy Search Algorithm (Left: no specification on the number of regions; Right: containing 11 regions)

Our computational results also suggest that the greedy search algorithm is likely to converge to a local optimum after approximately 30 iterations. Figure 6 shows the convergence of the algorithm with two different initial regional configurations, one of which is the current regional configuration and the other of which contains 58 single-OPO regions. Each iteration in the greedy algorithm takes about 3.5 minutes to search through approximately 200 regional configurations whereas each replication of the simulation takes 10 minutes to evaluate only one regional configuration. Hence, we concluded that the deterministic model is able to identify promising regional configurations with much less computational time.

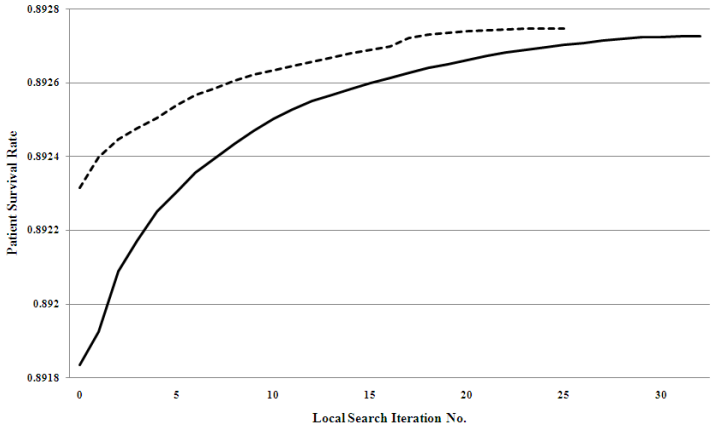

Figure 6: Greedy Search with Two Different Initial Regional Configuration (Solid Line: current; Dash Line: all regions are single-OPO regions)

5. CONCLUSIONS AND FUTURE RESEARCH

In this paper, we propose a deterministic model that represents the sequential liver allocation process with incorporation of patient waiting list dynamics. This model facilitates our analysis of the U.S. liver transplantation and allocation system. We use a simulation model as the benchmark to test the efficacy of the model in the problem of refining geographic distribution of procured livers. With the model, promising regional configurations can be efficiently identified without sacrificing much solution accuracy. Our computational results suggest that to improve patient survival rate, the region size should be reduced to certain extent.

The main limitation of the proposed deterministic model is that it does not consider the dynamics of each waitlisted patient's medical status. Such dynamics can be incorporated, which presumably leads to more accurate modeling. However, the computational time spent in evaluating one regional configuration may be significantly increased. In the future research, we plan to analyze the tradeoff between modeling validity and solution efficiency. At present, the solution method for the regional configuration optimization problem is still primitive. Another future research direction is developing more efficient local search methods for the regional configuration optimization problem in which the utility of each region is hard to compute.

REFERENCE

1. Alagoz, O. (2004). Optimal policies for the acceptance of living- and cadaveric-donor livers. Ph.D. thesis, University of Pittsburgh, Pittsburgh, PA.
2. Alagoz, O., Schaefer, A.J., and Roberts, M.S. (2009). Optimizing organ allocation and acceptance. In: P.M. Padalos and H.E. Romeijn (Eds.) Handbook of Optimization in Medicine,Springer, New York, NY, pp.1-21.
3. Demirci, M.C., Schaefer, A.J., Romeijn, H.E., and Roberts, M.S. (2010). An exact method for balancing efficiency and equity in the liver allocation hierarchy. Working paper.
4. Feng, W.X., Kong, N., and Wan, H. (2010). A simulation study of cadaveric liver allocation with a single-score ranking formula. Second revision submitted to ACM Transactions on Modeling and Computer Simulation.
5. Haymarket Media, Inc. (1998). State lawmakers approve organ-allocation bill. McKnight's Long-Term Care News, 20(11): 11.
6. Henderson, C.W. (2000). Waiting time drops for sickest patients under new liver policy. Transplant Weekly, May 28. Available from http://www.newsrx.com/newsletters/Transplant-Weekly/2000-05-28/2000052833317NW.html.
7. IoM – Institute of Medicine (1999). Organ Procurement and Transplantation: Assessing Current Policies and the Potential Impact of the DHHS Final Rule. National Academies Press, Washington, D.C.
8. Kamath, P.S., Wiesner, R.H., Malinchoc, M., Kremers, W., Therneau, T.M., Kosberg, C.L., D'Amico, G., Dickson, E.R., and Kim, W.R. (2001). A model to predict survival in patients with end-stage liver disease. Hepatology, 33(2): 464-470.
9. Kong, N. (2006). Optimizing the Efficiency of the United States Organ Allocation System through Region Reorganization. Ph.D. thesis, University of Pittsburgh, Pittsburgh, PA.
10. Kong, N., Schaefer, A.J., Hunsaker, B., and Roberts, M.S. (2010). Maximizing the efficiency of the U.S. liver allocation system through region design. Accepted for publication in Management Science.
11. Marcos, A., Fisher, R.A., Ham, J.M., Shiffman, M.L., Sanyal, A.J., Luketic, V.A.C., Sterling, R.K., and Posner, M.P. (1999). Right lobe living donor liver transplantation. Transplantation, 68(6): 798-803.
12. Organ Procurement and Transplantation Network / Scientific Registry of Transplant Recipients (2008). The 2008 OPTN/SRTR annual report: Transplant data 1998 - 2007. Available from http://www.ustransplant.org/annual reports/. Information accessed in August 2010.
13. Piratvisuth, T., Tredger, J.M., Hayllar, K.A., and Williams, R. (1995). Contribution of true cold and rewarming ischemia times to factors determining outcome after orthotopic liver transplantation. Liver Transplantation, 1(5): 296-301.
14. Pritsker, A.A.B., Martin, D.L., Reust, J.S., Wagner, M.A., Daily, O.P., Harper, A.M., Edwards, E.B., Bennett, l.E., Wilson, J.R., Kuhl, M.E., Roberts, J.P., Allen, M.D., and Burdick, J.F. (1995). Organ transplantation policy evaluation. In: Proceedings of the 27th Winter Simulation Conference, Arlington, VA. pp.1341-1323.
15. Ratcliffe, J., Young, T., Buxton, M., Eldabi, T., Paul, R., Burroughs, A., Papatheodoridis, G., and Rolles, K. (2001). A simulation modeling approach to evaluating alternative policies for the management of the waiting list for liver transplantation. Health Care Management Science, 4(2): 117-124.
16. Shechter, S.M., Bryce, C.L., Alagoz, O., Kreke, J.E., Stahl, J.E., Schaefer, A.J., Angus, D.C., and Roberts, M.S. (2005). A clinically based discrete-event simulation of end-stage liver disease and the organ allocation process. Medical Decision Making, 25(2): 199-209.
17. Simchi-Levi, D., Kaminsky, P., and Simchi-Levi, E. (2000). Designing and Managing the Supply Chain: Concepts, Strategies, and Case Studies. McGraw-Hill, New York, NY.
18. Stahl, J.E., Kong, N., Shechter, S.M., Schaefer, A.J., and Roberts, M.S. (2005). A methodological framework for optimally reorganizing liver transplant regions. Medical Decision Making, 25(1): 35-46.
19. Stahl, J.E., Kreke, J.E., Abdulmalek, F., Schaefer, A.J., and Vacanti, J. (2008). Consequences of cold-ischemia time on primary nonfunction and patient and graft survival in liver transplantation: A meta-analysis. PLoS ONE, 3(6).
20. State Legislatures (1999). Organ donations: Keep that liver at home (NCSL: The First 25 Years). July 1999.
21. The Economist Newspaper Ltd. (1998). Fighting over organs (federal-state controversy over allocation of organs for transplant). *The Economist*, 347(8066): 27.
22. Thompson, D., Waisanen, L., Wolfe, R., Merion, R., McCullough, K., and Rodgers, A. (2004). Simulating the allocation of organs for transplantation. Health Care Management Science, 7(4): 331-338.
23. Totsuka, E., Fung, J.J., Lee, M.C., Ishii, T., Umehara, M., Makino, Y., Chang, T.H., Toyoki, Y., Narumi, S., Hakamada, K., and Sasaki, M. (2002). Influence of cold ischemia time and graft transport distance on postoperative outcome in human liver transplantation. Surgery Today, 32(9): 792-799.
24. UNOS (2010a). United Network for Organ Sharing. Available from http://www.unos.org/.
25. UNOS (2010b). UNOS policy 3.6, Organ distribution: Allocation of livers. Available from

http://optn.transplant.hrsa.gov/PoliciesandBylaws2/policies/pdfs/policy 8.pdf
26. UNOS (2010b). UNOS data collection. Available from http://optn.transplant.hrsa.gov/data/.
27. Walter, J. (1998). Whose organs are they? Saturday Evening Post, 270(6), p. 70.
28. Wiesner, R.H., McDiarmid, S.V., Kamath, P.S., Edwards, E.B., Malincoc, M., Kremers, W.K., Krom, R.A., and R., W. (2001). MELD and PELD: Application of survival models to liver allocation. Liver Transplantation, 7(7): 567-580.
29. Xu, J., Kochanek, K.D., and Tejada-Vera, B. (2009). Death: Preliminary data for 2007. National Vital Statistics Report. Centers for Disease Control and Prevention.
30. Zenios, S.A., Chertow, G.M., and Wein, L.M. (2000). Dynamic allocation of kidneys to candidates on the transplant waiting list. Operations Research, 48(4): 549-569.

Appendix A. Model Notation

- Sequential Matching of A Single Procured Liver
  - $B'(l)$: ABO blood type of procured liver *l*
  - $G'(l)$: procurement OPO of *l*
  - $B(P)$: ABO blood type of waitlisted patient *p*
  - $G(P)$: registration OPO of *p*
  - $M(P)$: medical status of *p*
  - $G_i(l)$: OPO class relative to the procurement OPO of l (*i* = 1, local; *i* = 2, regional; *i* = 3, national)
  - M_i : medical status class (*i* = 1, acute; *i* = 2, sicker chronic; *i* = 3, less sick chronic)
  - $C(l)$: the set of immunologically compatible patients that are on the waiting list at the time liver *l* is procured
  - $C_i(l)$: the set of patients that are offered with liver *l* at step *i* of the sequential allocation process, *i* = 1,…, 9
  - $r_i(l)$: the probability that a patient at step *i* rejects l, *i* = 1,...,9
  - $P_i(l)$: the probability that *l* is accepted by some patient at step *i*, *i* = 1,...,9
  - $C_i(l, j)$: when *l* is procured, the set of patients in OPO *j*'s service area that may be offered with *l* at step *i*, *i* = 1,...,9
  - $P_i(l, j)$: the probability that *l* is accepted at step *i* by some patient in OPO *j*, *i* = 1,...,9

- Waiting List Update
  - *J*: the number of distinct procured liver categories
  - *K*: the number of distinct waitlisted patient categories
  - $x(t) = (x_1(t), x_2(t), ..., x_K(t))^T$: the number of patients in each category *k* =1,...,*K* at time $t \in [0,T)$
  - λ_k^+ ,: the rate with which transplant candidates of category *k* are added to the waiting list, *k* = 1,...,*K*.
  - μ_k : the rate with which transplant candidates of category *k* are removed from the waiting list due to reasons other than receiving transplants, *k* = 1,...,*K*.
  - $v_{jk}(t)$: at time $t \in [0,T)$, the likelihood that a category *j* liver is procured, allocated, and transplanted to a category *k* patient within the next unit time, *j* = 1,...,*J*, *k* = 1,...,*K*.
  - λ_j^- : the rate with which livers of category *j* are procured, *j* = 1,...,*J*.
  - $u_{jk}(t) : t \in [0,T)$, the instantaneous transplantation rate of category *j* livers to category *k* patients, *j* = 1,...,*J*, *k* = 1,...,*K*

- Regional Configuration Optimization
  - f : the post-transplant outcome accumulated over $[0,T)$
  - f_{jk} : the predicted post-transplant outcome of each transplant between a category *j* liver and a category *k* patient, *j* = 1,...,*J*, *k* = 1,...,*K*.
  - *r*: a region
  - *R*: a regional configuration, i.e., a partition of all OPOs
  - $f(R)$: the aggregate post-transplant outcome given regional configuration R
  - R : the set that contains all regional configurations
  - R' : the set that contains all regional configurations in which every region is contiguous

Appendix B. Expression of Waiting List Patient Subsets

Once a liver l is procured, $C(l)$ is the set that contains all patients that are on the waiting list. Then

- $C_1(l) = \{p \in C(l) \mid G(p) \in G_1(l), M(p) \in M_1\}$
- $C_2(l) = \{p \in C(l) \mid G(p) \in G_2(l), M(p) \in M_1\}$
- $C_3(l) = \{p \in C(l) \mid G(p) \in G_1(l), M(p) \in M_2\}$
- $C_4(l) = \{p \in C(l) \mid G(p) \in G_2(l), M(p) \in M_2\}$
- $C_5(l) = \{p \in C(l) \mid G(p) \in G_1(l), M(p) \in M_3\}$
- $C_6(l) = \{p \in C(l) \mid G(p) \in G_2(l), M(p) \in M_3\}$
- $C_7(l) = \{p \in C(l) \mid G(p) \in G_3(l), M(p) \in M_1\}$
- $C_8(l) = \{p \in C(l) \mid G(p) \in G_3(l), M(p) \in M_2\}$
- $C_9(l) = \{p \in C(l) \mid G(p) \in G_3(l), M(p) \in M_3\}$

Appendix C. A Simulation Model for the Liver Allocation System

The discrete-event simulation model used in this study was developed in Feng et al. (2010). It drew conceptual design ideas from the previous models such as UNOS Liver Allocation Model (ULAM) by Pritsker et al. (1995) and Liver Allocation Simulation Model (LASM) by Shechter et al. (2005).

The simulation was mainly calibrated by historic liver transplant data from the beginning of 2004 to the end of 2008. The model contains five modules: patient generation, donor generation, prioritization and matching, waitlist medical status update, and post-transplant relisting. The model is driven by the occurrence of five types of events: organ arrival and subsequent prioritization and matching, new patient arrival, medical status update, post-transplant graft failure and subsequent patient relisting, and post-transplant patient death. A flowchart of the model is presented in Figure 7. For a detailed description of each module, we refer to Feng et al. (2010). In the following, we outline the main differences between the deterministic sequential matching model developed in this paper and the simulation model.

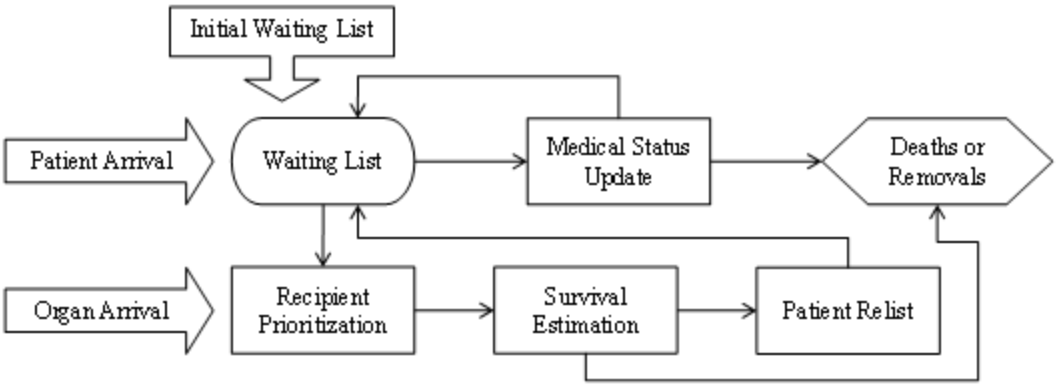

Figure 7: Diagram of a Liver Allocation Simulation Model (Feng et al., 2010)

In the simulation model, the stream of donor livers is generated probabilistically. The time when a donor liver is generated follows an annual stationary Poisson process. The distribution of liver category follows a discrete empirical distribution. Hence, a random number is drawn to determine which category the generated liver entity belongs to once the entity is created. The stream of new patient registrations is generated in a similar manner. Relisted patients are generated based on a decision whether the patient mortality or the graft failure occurs first at the post-transplant stage. Note that in the deterministic model, we do not differentiate relisted patient registrations and new patient registrations.

Once a liver entity is generated, the present patient waiting list is prioritized in a sequence identical to the one described in Section 2. In addition, waiting time is used to serve as tiebreakers. Although the assumption of proportional allocation may not be completely justified within each class in each replication, it can serve as a good proxy of liver allocation over a large number of replications.

In the simulation model, each patient's acceptance/rejection decision on a liver offer is modeled with a Bernoulli distribution. The acceptance/rejection probability is dependent upon the patient's medical status in the same way as the deterministic model. Hence, a random number is drawn to determine whether a particular patient would accept the

offer. Once a liver is accepted by a patient, the post-transplant 1-year patient survival rate is predicted through the same regression models as in the deterministic model.

With the input of the current regional configuration, we validated the model by comparing the simulated outcome with the corresponding historic data obtained from the 2008 OPTN/SRTR Annual Report (Organ Procurement and Transplantation Network / Scientific Registry of Transplant Recipients, 2008). Table 3 shows the comparison for year 2004 to 2006 (OPTN/SRTR did not report the patient survival rates in 2007 and 2008 in our latest access to their website). More validation results are reported in Feng et al. (2010).

Table 3: Simulation Model Validation w.r.t. Patient Survival Rate

	2004	2005	2006
Historic Rate	0.883	0.880	0.888
Simulated Mean	0.8918	0.8919	0.8917
Half Width of 95% CI	0.025	0.024	0.0032
Difference (Hist. vs. Sim.)	0.009	0.012	0.004

With the validation, we also identified the number of replications required to achieve a satisfactory level of statistic significance in terms of the studied system outcome. Figure 8 suggests that it is sufficient to run the simulation with 60 replications to predict the system outcome with the current regional configuration. We thus ran the simulation with 60 replications for alternative regional configurations to establish the validity of the deterministic model.

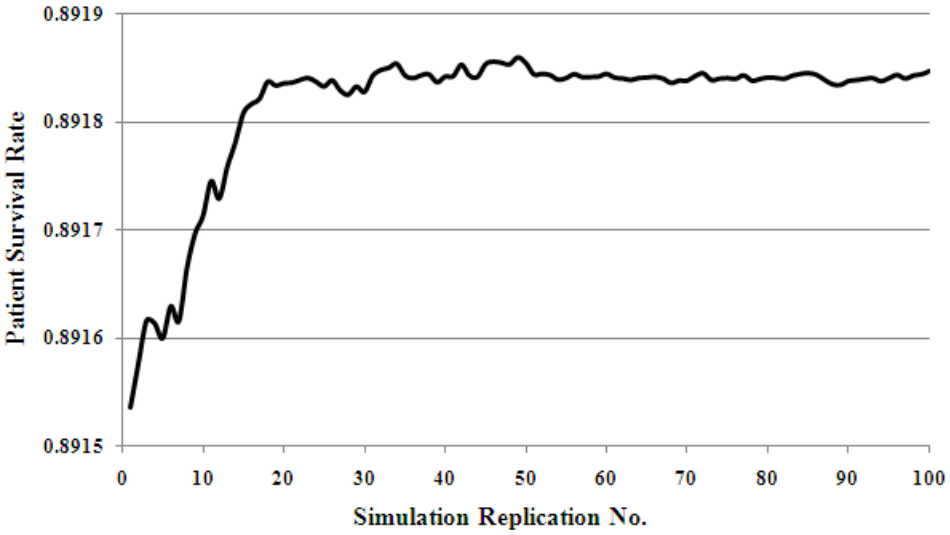

Figure 8: Average Simulated Outcome over Multiple Replications